AIMS Materials Science, 7(2): 182–191.
DOI: 10.3934/matersci.2020.2.182
Received: 17 January 2020
Accepted: 14 April 2020
Published: 06 May 2020

http://www.aimspress.com/journal/Materials

Research article

Evolution of intermetallic compounds in Ti–Al–Nb system by the action of mechanoactivation and spark plasma sintering

Yernat Kozhakhmetov[1,*], Mazhyn Skakov[2], Wojciech Wieleba[3], Kurbanbekov Sherzod[4], and Nuriya Mukhamedova[2]

[1] D. Serikbayev EKSTU, KZ-070000 Ust-Kamenogorsk, Kazakhstan
[2] National Nuclear Center of the Republic of Kazakhstan, KZ-071100 Kurchatov, Kazakhstan
[3] Wroclaw University of Science and Technology, PL-50-370 Wroclaw, Poland
[4] H.A. Yassawi International Kazakh-Turkish University, KZ-161200 Turkistan, Kazakhstan

* **Correspondence:** Email: kozhahmetov_e@nnc.kz; Tel: +77751316886.

Abstract: The present study shows promising approach to produce hydrogen-accumulated rechargeable intermetallic compounds (IMC) from three-component powder composition Ti–25Al–25Nb (at%), through experimentally chosen best modes and combined technological processes. The study includes research results on the effect of mechanoactivation (MA) process and following spark plasma sintering (SPS) technique on structural phase state of intermetallic Ti–Al–Nb composites. It was revealed that upon activation of the initial powder mixtures during their machining, intermetallic phases are formed by the interpenetration of aluminum into titanium and niobium lattices with the formation of solid solutions (Ti, Al) and (Nb, Al). It is found out, that the combination of MA and SPS is good for producing fine-graded predicted micro-structures in Ti–Al–Nb system owing to the activation of particle surface and formation of intermetallic phases at the preparation stage of powder mixture using MA technique as well as due to the effect of fast consolidation using SPS. This points to the fact of prospect for creating metal hydrides by combining MA and SPS techniques that makes it possible to obtain fine-grained IMC containing fair amount of O-phase.

Keywords: intermetallic compounds; Ti–25Al–25Nb alloy; spark plasma sintering; mechanoactivation; O-phase

1. Introduction

So far, efforts are underway to study IMC based on titanium aluminides with high content of Niobium. Ti_2AlNb-based materials belong to the third generation of titanium aluminides and have an orthorhombic basocentric crystal lattice. A wide homogeneity range of these intermetallics confers the possibility to produce the materials with different chemical composition. Intermetallic Ti–Al–Nb composites own interesting structural properties; they are hydride-forming and are able to absorb hydrogen extensively that provides them with a significant advantage while using them as hydrogen storage materials [1,2].

Low density, safety and wide distribution of these elements make them especially attractive. However, at the moment one of the main problems of the development of this direction is the lack of reliable manufacturing technology for producing the Ti_2AlNb-based IMC, which could provide the best properties depending on the purpose. The present study showed that structural-phase state and physical-mechanical properties of Ti_2AlNb-based IMC can be controlled directly by the production technology [3,4].

The application of the MA technique at the stage of powder mixture preparation creates active states in a solid body, opening a certain prospect for subsequent conducting and accelerating chemical reactions between the solid bodies and producing materials in a high-equilibrium state. Activation of solids bodies in the course of their mechanical processing by grinding in shock, shock-abrasion or abrasion modes leads to the accumulation of structural defects, increase in curvature and surface area, phase transformations and even amorphization of crystals, thus affecting their chemical activity [5,6].

At the same time, during the last decade there were published a number of studies considering the application of powder sintering technique in spark plasma [7]. Short-term high-temperature effect on powder mixture, optimal ratio of heating and deformation modes of the material, as well as the way of electric current through the powder mixture allow to obtain high-strength materials characterized by a fine-grained structure, low porosity and low mechanical stresses [8,9]. New composites with best properties might be produced in case of realization of this technology.

As reviewed above, the combination of MA and SPS techniques can strike out in an original direction of consolidation of Ti–Al–Nb alloys. Few research works have experienced in this issue, so the effect of sintering process on the structure, phase state and physical and mechanical properties of Ti–Al–Nb alloys should be investigated further. The effect of MA on the process of consolidation of powder mixture is also reasonably to study.

This study aims and focuses on the effect of preliminary MA and subsequent SPS on the structural-phase state of intermetallic compound in the Ti–Al–Nb composite.

2. Materials and methods

The studied intermetallic compounds in the Ti–25Al–25Nb composite (at%) have been produced through the combination of two techniques: MA and SPS. Titanium powder with particle size of 45–60 μm, Niobium powder with particle size of 40–63 μm, and Aluminum powder were used as a reference material. Aluminum powder of different dispersity and morphology were used in order to assess the impact of the properties of the initial powder on the final product:

- Aluminum nanopowder with fuzzy-edged particles of ~90–250 nm. The powder is heavy

agglomerated.

- Aluminum powder is characterized with quite different size of the particles from 50 to 60 μm. The particles are mostly globular.
- The particles of aluminum chips have compacted and dominant sponge structure. Size of the aluminum chips' particles is in the range of 100–150 μm.

The powders were mixed up in a P100CM planetary mill at the ratio of the masses of moldering bodies with a diameter of 10 mm to the processed material as 23:1 than they were subjected to the MA. Table 1 provides details of the MA.

Table 1. Details of the MA.

	Materials	Duration (min)	Rotation velocity (rpm)	Changing the direction of rotation of the planetary disk (min)	Testing environment	The degree of grinding Al in the initial mixture
Mixin	Ti–Al–Nb	35	250	–	Argon	
MA	Ti–Al–Nb mixture	20	650	–	Argon	Nanopowder
	Ti–Al–Nb mixture					Powder
	Ti–Al–Nb mixture					Shavings
	Ti–Al–Nb mixture	180	350	every 30		

The morphology and particle size distribution of mechanically activated powders, as well as the microstructure and elemental composition of the obtained IMC were studied in the topographic and compositional contrast mode using scanning electron microscope TescanVega3 with the addition of energy dispersion spectral analysis. X-ray phase analysis (XPA) of studied materials was performed in X-ray diffractometer Empyrean in Cu-Kα radiation. Ready diffractograms were processed in the HighScore program.

The SPS of powder mixtures was carried out in the vacuum (10^{-5} Pa) in SPS-515S machine (SyntexInc., Japan). The powder mixture was consolidated under the temperature of 1300 ºC, static pre-pressing pressure of 20 MPa and isothermal exposure for 5 min.

Integrated video cameras recorded some changes in linear dimensions of ceramic material in the course of the sintering process. A high-temperature pyrometer, built-in a technological hole in the side wall of the mold, measured the temperature in the course of the sintering process which ranged from 575 to 2500 °C.

3. Results and discussions

3.1. Mechanoactivation

Detailed analysis of the radiographs of powder mixture after MA has shown it is quite complicate to identify phase composition because of the overlapping most strong lines of the phases.

However, when the MA process lasted for 20 min, regardless the size of their aluminum particles, each powder mixture showed the main peaks of single elements like Ti, Al and Nb. This justifies that the mixture contains unreacted particles.

According to the analysis results of diffractograms α-Ti with hexagonal crystal lattice of the spatial group P63/mmc, Nb with a body-centered cubic lattice (bcc) of the spatial group Im3m, Al with a cubic lattice, the spatial group Fm-3m are common phases for the composition of samples of all powder mixtures. Figure 1 shows the overlapping of diffractograms of powder mixture Ti–Al–Nb.

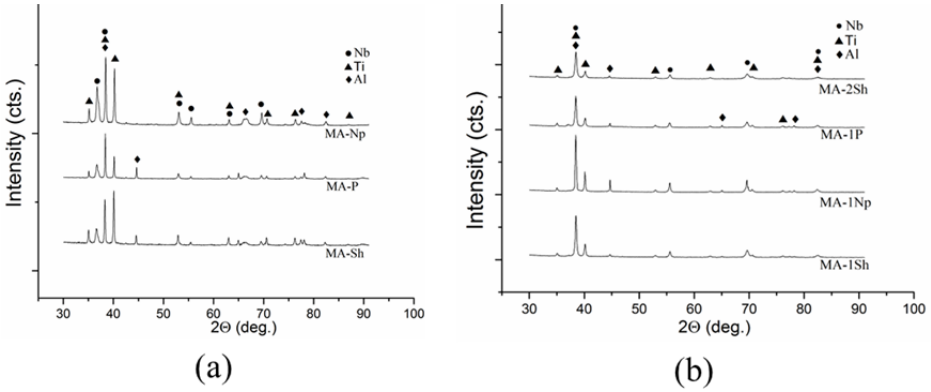

Figure 1. Diffraction pattern of the mixture Ti–Al–Nb: (a) in the initial state, (b) after MA in different modes.

While studying diffractograms it was stated that intensity line and width of peaks depend on the MA process and size of aluminum particles. Maximum intensity of peaks of aluminum phase after the MA process is observed on the diffractograms of MA-1Np mixture, whereas the opposite effect is observed for MA-1P mixture: diffraction peaks Ti, Al and Nb decreased in intensity and expanded in width. The same case is typical for MA-2Sh powder mixture after 180 min since the MA has started. Sim et al. [10] studied that this is due to the process of synthesis of metastable supersaturated solid solutions by mixing elementary powders at MA powder mixture of Ti–Al–Nb system. Therefore, after the MA process, when using MA-1P mixture for 20 min and MA-2Sh mixture for 180 minutes, most of aluminum particles were dissolved in the lattice Ti and Nb by interpenetration with formation solid solutions (Ti, Al) and (Nb, Al). In addition, Mukhamedova et al. [11] studied that in the process of sample preparation by the MA technique the orthorhombic phase Ti_2AlNb is also formed and by increasing of MA duration the composition of this phase will only raise [12].

Scanning electron microscopy of mechanically activated powder mixtures in the topographic and compositional contrast mode showed that as a result of multiple effects of cold welding of Al, Ti, Nb and destruction we can observe formation of layered composite particles. In case of using MA-1Np mixture with aluminum nanopowder after treatment for 20 min (Figure 2a) there is a sticking of aluminum on titanium and niobium particles, without formation of solid solution, that explains maximum intensity of peaks of aluminum phase after MA.

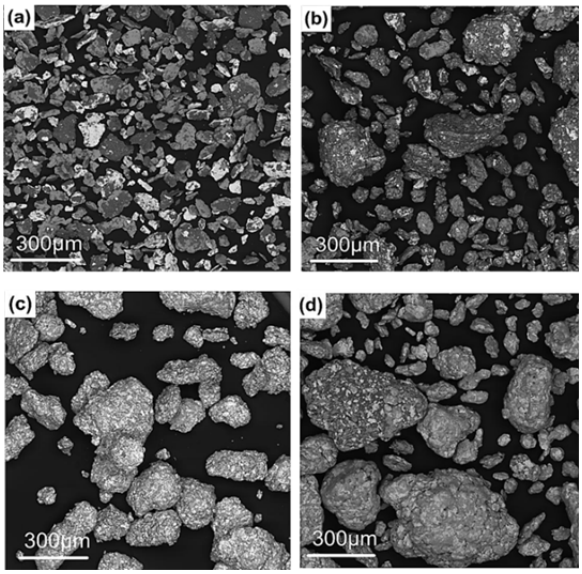

Figure 2. SEM image of Ti–25Al–25Nb (at%) alloy powder particles after MA: (a) sample MA-1Np, (b) sample MA-1P, (c) sample MA-1Sh, and (d) sample MA-2Sh.

It was found that after MA, the powder particles become inhomogeneous and polyhedral-shaped. With extending time of the MA process we can observe a gradual transformation of the particle shape into a spherical one that is mainly characterized for small particles. Figure 3 and Table 2 show results of EDS analysis of particle's local regions after cold welding effect.

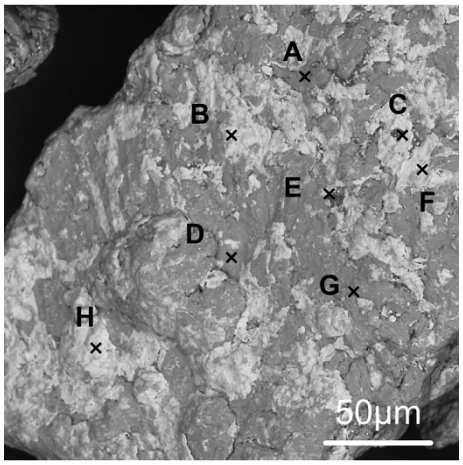

Figure 3. SEM image and EDS analysis of particle of powder mixture MA-2Sh after MA for 180 min.

Table 2. Results of local element analysis of powder mixture MA-2Sh in weight shares.

Title	Al	Ti	Nb	Title	Al	Ti	Nb
A	13.06	71.20	15.75	E	76.14	7.20	16.66
B	6.37	4.30	89.33	F	6.22	11.82	81.96
C	70.11	9.16	20.73	G	11.05	81.02	7.93
D	6.65	88.53	4.82	H	16.58	28.26	55.16

As can be seen in Figure 3, regions with a dark grey tint are typical for areas with high titanium content, whereas the areas of light gray tint are typical for the regions with high content of niobium. According to the results of EDS-analysis of local points, it can be said that the fractions of powder mixtures are inhomogeneous in each single particle and consist of areas enriched or depleted with titanium and niobium. In this case, aluminum is almost completely dissolved, except of some local areas. At the same time, composition of predominant and secondary initial components varies in a wide range of values.

Nowadays it has been inferred that characteristics of the feedstock mostly determine microstructure, phase composition and operating properties of sintered solid alloys and intermetallic compounds. Many researchers have introduced studies on the effect of characteristics of initial powders on the structure and properties of solid alloys [13]. Morphology and size of particles of powder mixture of Ti–Al–Nb system directly impact on the structure and operating properties of producing material while their consolidation. This is due to nonequilibrium and chemical inhomogenuity of poly-phase particles as well as diffusion velocity while sintering.

The analysis of particle size showed that particles are randomly distributed throughout the mixture (Figure 4). Such distribution is caused by multiple plastic deformations of particles, their cyclic conglomeration and destruction that results in increase of small and large fractions after MA process. As can be seen in Figure 3, powder mixtures with aluminum chips MA-1Sh and MA-2Sh with a particle size of more than 100 μm are the most susceptible to particle conglomeration. Fractions with size of more than 300 μm are not detected for a mixture using aluminum powder and nanopowder herewith. It is seen, that particle conglomeration depends on duration of MA process because constant activation of particle surface takes place with increasing MA time that, in turn, leads to cold welding of these particles.

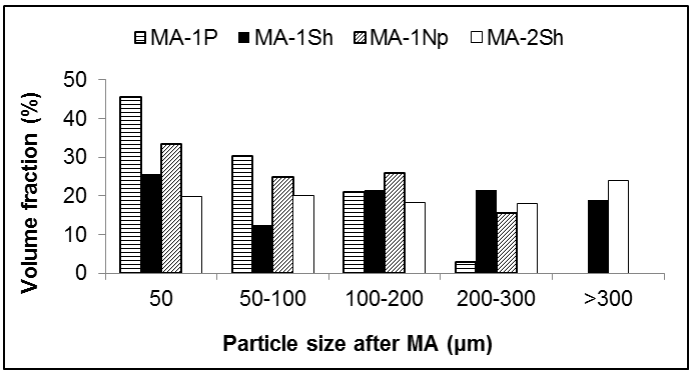

Figure 4. Distribution of particles on sizes after MA process.

3.2. Microstructural research of intermetallic Ti–Al–Nb composites by combining of MA and SPS techniques

The temperature of SPS was experimentally identified according to the phase diagram of Ti–Al–Nb system. Samples sintered under the temperature of 1300 °C are characterized by a homogeneous multiphase structure consisting of intermetallic Ti_3Al, $AlNb_2$, B2 and O-phases, without pores and cracks. The characteristic structure of sintered samples and the results of local elemental analysis are shown in Figure 5 and Table 3.

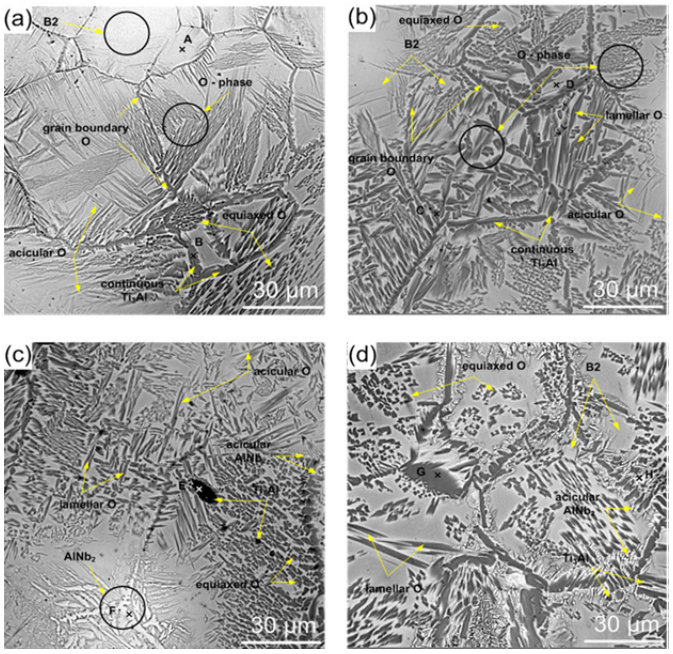

Figure 5. SEM image and XPA of samples based on Ti–25Al–25Nb system (at%)) after SPS under 1300 ºC/5 min/20 MPa: (a) sample MA-2Sh, (b) sample MA-1P, (c) sample MA-1Np, and (d) sample MA-1Sh.

Table 3. Results of local element analysis of IMC samples after SPS in weight shares.

Title	Al	Ti	Nb	Phase	Title	Al	Ti	Nb	Phase
A	15.87	56.37	27.75	B2	E	22.08	68.55	9.37	Ti_3Al
B	25.83	51.03	23.14	O	F	13.62	19.50	66.89	$AlNb_2$
C	13.96	57.38	28.66	Ti_3Al	G	28.14	50.42	21.44	O
D	29.52	58.47	12.02	B2	H	13.01	19.25	67.74	$AlNb_2$

Review of microstructure of sintered samples under the temperature of 1300 ºC revealed noticeable changes in distributions and in the contents of the main phases. This is evidenced by the images of the surface of the samples obtained by the SEM method. Figure 5 shows SAM images of Ti–25Al–25Nb alloys (at%). It is seen that in the samples, sintered under the temperatures of 1300 ºC, almost complete diffusion of unreacted Niobium and titanium occurs, while the grain boundaries of B2 phase are noticeably enlarged on all samples. This is probably due to the decay of most part of Ti_3Al phase, which is forming in the course of the sintering. It likely seems that at the sintering stage, the niobium element quickly diffuses and penetrates the intergranular boundary of Ti_3Al, and the phases with a large average size of Ti_3Al are broken into many small globular particles and deposited at the boundaries of B2 phase [14]. In addition, Niobium and Aluminum occupy Ti positions in B2 phase and form O-phase at the grain boundaries. Thus, the microstructure of the samples under the given temperature consists mainly of the B2 + O phase, and composition becomes more homogeneous. However, as can be seen in Figures 5b,c at the grain boundaries of B2 phase, there are still intermittent globular deposition and long aligned Ti_3Al phase bars, which are located parallel to the grain boundary of B2.

It is worth noting that distribution of $AlNb_2$ phase on the surface of the samples while sintering

under the temperature of 1300 ºC led to the formation of a coarse-crystalline dendritic structure for this phase. $AlNb_2$ phase distribution has two features. The main part of particles are plate-shaped and look like needles up to 5 μm thick and 20–25 μm long in the field of metallographic sections and located mainly at the triple joints of B2 phase (Figure 5c), and grow as needles into the grain bodies and B2 phase boundaries. We also can observe accumulation of this phase in the form of short needlelike inclusions distributed throughout the diameter of B2 grains (Figure 5d), which create a barrier with a thickness of 4–5 μm between the main B2 phase and boundary O-phase.

If the first type of distribution of $AlNb_2$ phase is typical for all samples, the second type is mostly related to sample MA-1Sh. It might be due to short-term technological processes (MA and SPS) and worse diffusion feature. Residual niobium in powder mixture MA-1Sh cannot complete reactive diffusion and deposit as $AlNb_2$ phase.

As shown from Figure 5, microstructure of samples under this sintering temperature is characterized by the presence of plate-like structure of O-phase 10–25 μm long and 5–6 μm thick. At the same time there are globular accumulations of O-phase from 2 to 5 μm in some areas. O-phase distribution depends on the size of Al particles in the initial burden and pre-Ma modes. For example, MA-1Sh sample is characterized by globular accumulation of O-phase in the grain body of B2 phase which sizes vary widely. MA-1P and MA-1Np samples are characterized by wide lamellar structure and globular accumulation of O-phase sized less than 2 μm. It should be emphasized that these two types of O-phase can be found in separate B2 phase grains and at the same time can be combined in one B2 phase grain matrix. MA-2Sh sample, where MA process was carried out for 180 minutes, differs from other samples by the absence of above mentioned types of O-phase distribution, and it is characterized by the presence of lamellae in the grain body, which are located perpendicular to the grain boundaries of B2 phase and have different lengths and widths. Changes in the volume fractions of the O-phase between different samples are shown in Figure 6. As can be seen from the Figure, while SPS under the temperature of 1300 ºC, B2-phase and O-phase are the main ones for all samples, at the same time there is a small amount of Ti_3Al-phase. Identifying of the volume fraction of $AlNb_2$-phase was difficult due to their small content and local distribution. The O-phase content for all samples is the highest in comparison with other phases and reaches a maximum on the MA-2Sh sample at a value of 50.92%. This dependence of O-phase is typical for all samples regardless of particle size and MA duration. This indicates that the O-phase is rapidly precipitated from B2 and Ti_3Al phases.

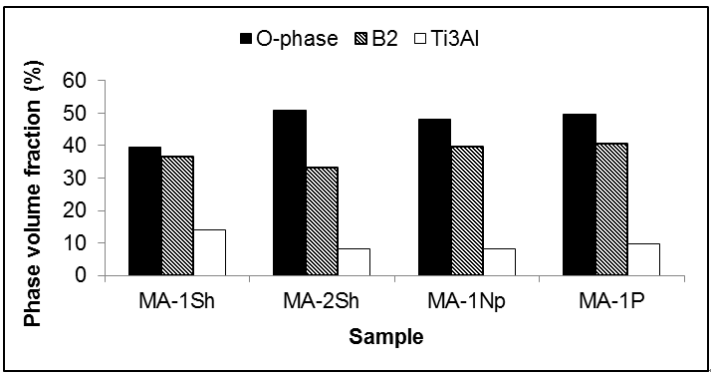

Figure 6. Changes of volume share of O-phase in samples depending on particle size and MA duration.

Longer duration of the MA has positive impact on IMC structure especially on the formation of O-phase. Increase in time of MA for MA-2Sh sample led to more homogeneous distribution of O-phase which characterized with fine texture of lamellae, whereas the samples obtained after 20 min since MA has started are more heterogeneous. This is due to the formation of solid solution BCC (Ti, Al, Nb) and its increased content because of longer MA.

4. Conclusion

The following conclusions were made throughout this work:

–Intermetallic phases are evolving in the process of MA of initial powder mixtures due to aluminum penetration in the Ti and Nb grids and owing to formation of solid solutions (Ti, Al) и (Nb, Al);

–Extending time of MA gives positive effect on the structure of new intermetallic compounds. This is due to formation of solid solution BCC (Ti, Al, Nb) and its increased content while the time extending of the MA;

–By combining MA amd SPS processes it is able to monitor structural-phase state of the final product. For example, MA-1Sh specimen is characterized by globular accumulations of O-phase in the body of the grain of B2-phase. Specimens MA-1P and MA-1Np are characterized by lamellar structure and globular accumulation of O-phase no more than 2 μm. Specimen MA-2Sh, where MA lasted for 180 min, differs from other specimens because it hasn't above characteristics with more homogenous distribution of lamellae of O-phase in the body of the grain of B2-phase located up-and-down the boundaries of the grains;

–Lastly through the conclusions as mentioned above, it was proved that the combination of MA and SPS techniques makes it possible to produce fine-grained predicted microstructures in Ti–Al–Nb system. This is due to the activation of particle surface and the formation of intermetallic phases at the preparatory stage of powder mixture using MA as well as due to rapid consolidation reached by SPS. This is promising direction to produce metal hydrides using MA and SPS in order to obtain fine-grained IMC with required amount of O-phase.

Acknowledgments

The work has been implemented within the framework of the scientific and technical program "Development of nuclear energy in the Republic of Kazakhstan for 2018-2020" on the theme "Study of advanced materials based on Ti–Al–Nb system for hydrogen storage and transportation".

Conflict of interests

The authors declare that there is no conflict of interests regarding the publication of this paper.

References

1. Polozov I, Sufiiarov V, Kantyukov A, et al. (2019) Selective laser melting of Ti_2AlNb-based intermetallic alloy using elemental powders: effect of process parameters and post-treatment on microstructure, composition, and properties. *Intermetallics* 112: 106554.

2. Karakozov BK, Skakov MK, Kurbanbekov SR, et al. (2018) Structural and phase transformations in alloys during spark plasma sintering of Ti + 23.5 at% Al + 21 at% Nb powder mixtures. *Inorg Mater* 54: 37–41.
3. Niu HZ, Chen YF, Zhang DL, et al. (2016) Fabrication of a powder metallurgy Ti_2AlNb-based alloy by spark plasma sintering and associated microstructure optimization. *Mater Design* 89: 823–829.
4. Appel F, Clemens H, Fischer FD (2016) Modeling concepts for intermetallic titanium aluminides. *Prog Mater Sci* 81: 55–124.
5. Luo L, Liu T, Li K, et al. (2016) Microstructures, micro-segregation and solidification path of directionally solidified Ti–45Al–5Nb alloy. *China Foundry* 13: 107–113.
6. Wu J, Xu L, Lu Z, et al. (2015) Microstructure design and heat response of powder metallurgy Ti_2AlNb alloys. *J Mater Sci Technol* 31: 1251–1257.
7. Maniere C, Lee G, Olevsky EA (2017) All-materials-inclusive flash spark plasma sintering. *Sci Rep* 7: 15071.
8. Bauri R, Chaudhari R (2014) Microstructure and mechanical properties of titanium processed by spark plasma sintering (SPS). *Metallogr Microst Anal* 3: 30–35.
9. Chen X, Xie FQ, Ma TJ, et al. (2015) Microstructure evolution and mechanical properties of linear friction welded Ti_2AlNb alloy. *J Alloy Compd* 646: 490–496.
10. Sim K, Wang G, Son R, et al. (2017) Influence of mechanical alloying on the microstructure and mechanical properties of powder metallurgy Ti_2AlNb-based alloy. *Powder Technol* 317: 133–141.
11. Mukhamedova NM, Kozhakhmetov YeA, Skakov MK, et al. (2019) Effect of mechanoactivation on the formation of O-phase in Ti–Al–Nb system. *Bulletin KazNITU* 5: 115–120.
12. Salvo C, Chicardi E, García-Garrido C, et al. (2019) The influence of mechanical activation process on the microstructure and mechanical properties of bulk Ti_2AlN MAX phase obtained by reactive hot pressing. *Ceram Int* 45: 17793–17799.
13. Voisin T, Monchoux JP, Couret A (2019) Near-net shaping of titanium–aluminum jet engine turbine blades by SPS, In: Cavaliere P, *Spark Plasma Sintering of Materials: Advances in Processing and Applications*, Cham, Switzerland: Springer, 713–737.
14. Kurbanbekov ShR, Skakov MK, Baklanov VV, et al. (2017) Effect of spark plasma sintering temperature on structure and phase composition of Ti–Al–Nb based alloys. *Mater Test* 59: 1033–1036.

AIMS Press